ISBN: 978-3-95450-247-9 ISSN: 2673-5490 doi: 10.18429/JACoW-IPAC2024-TUPS01

STUDY OF LONGITUDINAL EFFECTS DURING TRANSITION CROSSING OF THE EIC HADRON STORAGE RING*

H. Lovelace III†, K. Drees, S. Peggs, V. Ptitsyn
Brookhaven National Laboratory, Upton, NY, USA
R. Seviour, University of Huddersfield, Huddersfield, UK

Abstract

The Electron Ion Collider (EIC) Hadron Storage Ring (HSR) will accelerate all species except protons through transition to the desired storage energy. The effects at transition may cause unwanted emittance blowup beam loss due to bunch area mismatch and negative mass instability. In this paper, we will show the longitudinal dynamics of transition crossing in the HSR with current parameters using the accelerator code Beam Longitudinal Dynamics (BLonD).

INTRODUCTION

The Electron Ion Collider will provide collisions of center-of-mass energy above 130 GeV. Energetic nuclear collision at HERA [1] proved the gluon dominance within the hadron nucleus. The primary goal of the EIC is to answer fundamental questions of nucleon spin contribution, nucleon mass, and dense systems of gluons [2]. The EIC will probe with highly polarized electron beam, the polarized and unpolarized nucleus of hadron beams to find understanding in the correlations of the sea quarks and gluon contribution to the nucleon spin [3]. In addition to understanding the polarization of the atomic nucleus, the EIC will explore the regime of gluon saturation in the quest to understand color propagation through the nucleus using the electron/Proton Ion Collider (ePIC) detector [4].

The polarized electrons will be provided by a polarized electron gun similar to the Stanford Linear Collider source [5]. The beam will be injected into a 200 MeV linear accelerator (LINAC) through a transfer line containing a spin rotator that places the spin direction of the electron vertically, into a Rapid Cycling Synchrotron (RCS) booster. Ramping to 3 GeV in the booster, the beam is injected into the RCS and ramped to energy to matched the electron storage ring energy which ranges from 5 GeV to 18 GeV.

For the hadron accelerator chain, the sources will be the Optically Pumped Polarized Ion Source [6] and the extended Electron Beam Ion Source (EBIS) [7]. From the OPPIS the beam is accelerated to 200 MeV and injected into the Alternating Gradient Synchrotron (AGS) booster. The EBIS injects directly into the booster. The booster accelerates the beam to magnetic rigidity of 17 Tm [8] then extracts into the AGS. The AGS accelerates the beam to a maximum rigidity of 82 Tm and extracts into the Hadron Storage Ring (HSR).

* Work supported by Brookhaven Science Associates, LLC under Contract No. DE-SC0012704 with the U.S. Department of Energy.
† hlovelace3@bnl.gov

Transition

Since 1949, transition crossing in closed geometry accelerators has been studied [9]. The first accelerator to cross transition was the 10 MeV "electron analog" of the AGS [10] located at Brookhaven National Laboratory. To reach high energies, all species except for protons must cross transition energy in the HSR [11]. Transition is essentially the reduction of the longitudinal motion at the energy where all particles have the same period. At that energy, the motion of the beam becomes unstable. The Lorentz factor, γ, of the beam at transition is

$$\gamma_T = 1/\sqrt{\alpha_c} \tag{1}$$

where,

$$\alpha_c = \oint ds(\eta_x/\rho_x) = \frac{\Delta C/C}{\delta_p} \tag{2}$$

The momentum compaction, α_c, is a factor that is applied to a given bending radius of a dipole, ρ or momentum spread, δ_p, that describes the change in dispersion, η_x and circumference change, $\Delta C/C$, of the particle trajectory over the entire ring, ds. The slippage, η_s, is defined as

$$\eta_s = \alpha_s - 1/\gamma^2 \tag{3}$$

where it is clear to see that if $\eta_s < 0$, the particles that have higher momentum will have a higher revolution frequency, and if $\eta_s > 0$ the particles that have lower momentum will have a lower revolution frequency therefore at transition the revolution frequency of the particles is independent of the particles energy. This effect, in turn, reduces the bunch length increasing the peak current and space charge effects. At transition, $\eta_s = 0$ and the bunch length is at a minimum. The synchrotron tune begins to slow and the beam becomes nonadiabatic as transition is approached. The adiabticity condition,

$$\Omega = \frac{1}{\omega_s^2}\left|\frac{d\omega_s}{dt}\right| \ll 1 \tag{4}$$

where is the angular frequency and t is time [12]. In Equ. 4, it is clear that there is no change in the action provided that $\Omega \ll 1$ [13]. The time period in which the beam becomes nonadiabatic is defined as [14]

$$T_C = \left(\frac{AE_T}{ZeV|\cos(\phi_s)|} \times \frac{\gamma_T^3}{h\gamma'} \times \frac{C^2}{4\pi c^2}\right)^{1/3} \tag{5}$$

where A is the atomic weight, Z is the atomic number, E_T is the transition energy, e is the charge of the electron, V

ISBN: 978-3-95450-247-9 ISSN: 2673-5490 doi: 10.18429/JACoW-IPAC2024-TUPS01

is the RF cavity voltage, γ_T is the transition γ, h is the harmonic number, and $\gamma' = d\gamma/dt$. The "nonlinear momentum compaction factor", α_1 is defined as [15]

$$\delta L/L_0 = \alpha_c \delta(1 + \alpha_1 \delta + ...) \tag{6}$$

where L_0 is the circumference of the lattice. For all particles within a bunch to have the same γ_T, $\alpha_1/\alpha_c = -1/2$. If $\alpha_1/\alpha_c = -3/2$, the particles within the bunch cross transition at the same time [16].

Transition Crossing in HSR

Using the accelerator code Beam Longitudinal Dynamic (BLonD) [17], the HSR transition crossing was modeled with the parameters shown in Table 1. The HSR will use the existing 28 MHz cavities of the RHIC [18] detuned to the 315 harmonic. The change in harmonics is due to the change in the number of bunches injected into the HSR (290) compared to RHIC (110) and the reuse of the 197 MHz normal conducting storage cavities. The HSR will also utilize the First Order Matched [15] transition jump scheme which was first implemented in RHIC. For the synchronous phase, ϕ_s, matching pre- and post-transition,

$$\phi_s = \sin^{-1} \frac{\Delta E}{ZeV_{rf}} \tag{7}$$

where as the energy gain per turn, ΔE. A phase jump of $180 - \phi_s$ necessary at transition for bunch area matching after transition. Figures 1 (pre-transition), 2 (transition), and 3 (post-transition), are plots of the longitudinal phase space. Notice the tilt to the phase space ellipse that is present at transition.

Table 1: Transition Parameter Table

Parameter	Value
Species	Au^{79}
γ_T	23.08
Ramp rate, γ' (s^{-1})	0.4
Voltage, V (kV)	200
Harmonic (#)	315
Synchronous Phase, ϕ_s (rad)	0.06
Characteristic Time, T_c (ms)	69.85
Nonlinearity parameter, α_1 ($\times 10^{-4}$)	-4.21

The separatrix from the RF can written as

$$\begin{aligned} \Delta E_{n+1} &= \Delta E_n + eV(\sin\phi_n - \sin\phi_s) \\ \phi_{n+1} &= \phi_n + \frac{2\pi h\eta}{\beta^2 E}\Delta E_{n+1} \end{aligned} \tag{8}$$

The RMS longitudinal emittance (eVs) and longitudinal *beta*-function, β_z is

$$\begin{aligned} \epsilon_z &= \pi\sigma_E\sigma_t \quad \text{RMS emittance} \\ \beta_z &= \frac{C}{2\pi}\frac{|\eta|}{Q_s} \end{aligned} \tag{9}$$

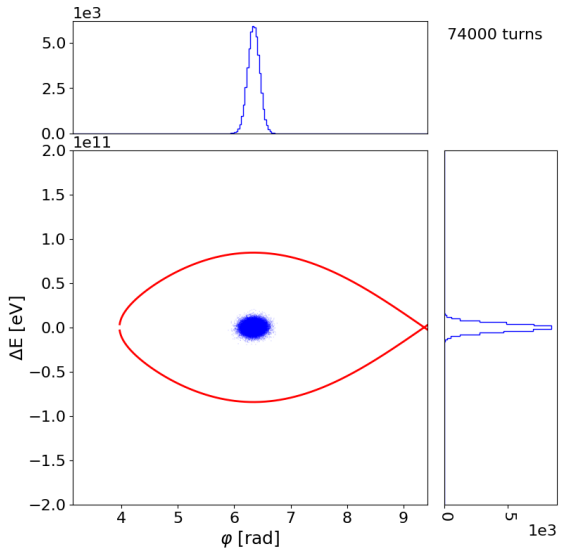

Figure 1: Pre-transition bunch and accelerating RF-bucket below transition. The red curve is the RF bucket and the points are the macroparticles. The horizontal and vertical axes are ϕ_s, the synchronous phase angle of the particle and ΔE, energy spread of the bunch. The beam profile of the phase (top) and the energy (right) amplitudes are in arbitrary units.

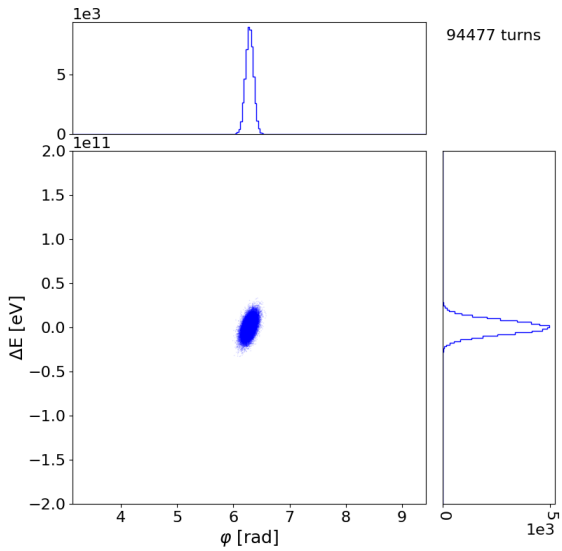

Figure 2: At transition, excluding the effects of the nonlinearities, the bunch is stretches and tilts. After transition, if well matched, the bunch returns to the pre-transition orientation. The points are the macroparticles with the axes ϕ_s the synchronous phase angle horizontal, and ΔE the energy spread vertical. The beam profile of the phase (top) and the energy (right) amplitudes are in arbitrary units.

RESULTS

Figure 4 shows the effect of varying the γ' through transition from $\Delta\gamma = \gamma_T \pm 0.5$. It clear that by ramping quickly through transition, the effects of transition on the bunch

ISBN: 978-3-95450-247-9 ISSN: 2673-5490 doi: 10.18429/JACoW-IPAC2024-TUPS01

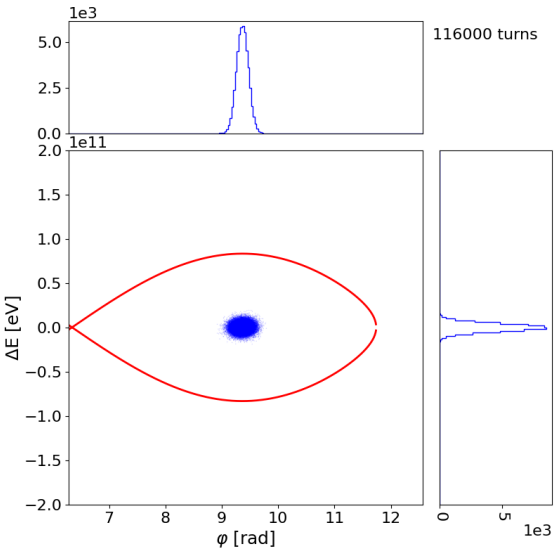

Figure 3: Post-transition bunch and accelerating RF-bucket below transition. The red curve is the RF bucket and the points are the macroparticles. The horizontal and vertical axes are ϕ_s, the synchronous phase angle of the particle and ΔE, energy spread of the bunch. The beam profile of the phase (top) and the energy (right) amplitudes are in arbitrary units.

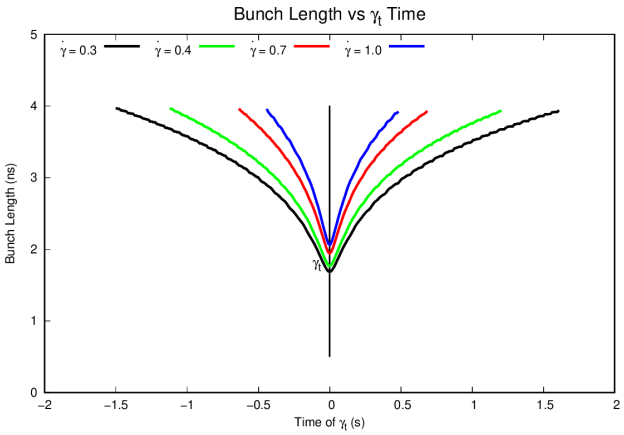

Figure 4: Bunch length vs time of transition crossing with various ramp rates ($\dot{\gamma} = d\gamma/dt$). The revolution frequency is 78 kHz. The vertical line indicates transition crossing.

length is mitigated. The ramp rate of the HSR will be similar to RHIC, where the expected value of γ' = $0.4s^{-1}$ which gives the a minimal bunch length of 1.765 ns which is 0.53 m. Figure 5 shows the effect of transition on the energy spread and bunch length with the standard RHIC ramp rate. At transition, the energy spread is at a maximum. The vertical purple lines of Fig. 5 indicate the beginning and end of the nonadiabatic region of the ramp. The emittance in Fig. 6, increases during this time period and returns to the pre-transition value after [12]. This growth is correlates to the tilt of the ellipse seen in Fig. 2.

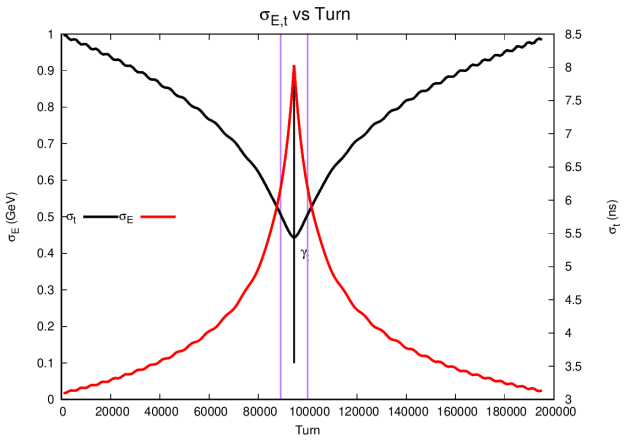

Figure 5: A plot of $\sigma_{E,t}$ vs turn. The black vertical line indicates transition crossing. The purple lines mark the beginning and end of the nonadiabatic region.

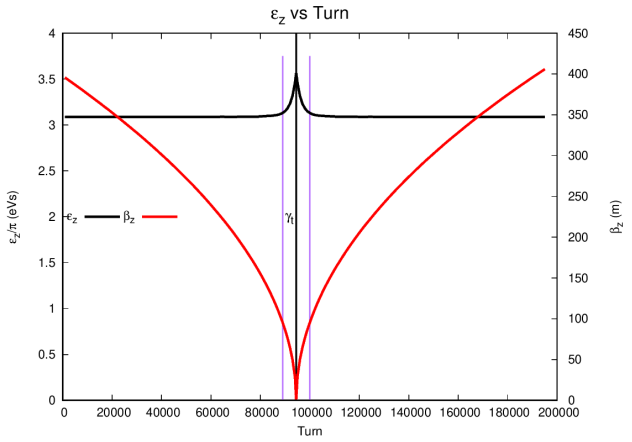

Figure 6: A plot of ϵ_z vs turn. The black vertical line indicates transition crossing. The purple lines mark the beginning and end of the nonadiabatic region.

CONCLUSION

The current ramp rate of the 0.4 s^{-1} seems to be sufficient in crossing transition with a 30% variation within the ramp rate from 0.3 s^{-1} to 1.0 s^{-1}. The bunch length minimum during transition in the absence of impedance is 1.9 ns. The nonadiabtic time for a ramp of 0.4 s^{-1} is 69.85 ms. To fully model the effect of transition, an impedance model is needed to give an accurate account bunch area matching pre- and post-transition. A full 6D model will also provide transitional effect longitudinally in concert with the transverse optical manipulation of γ_T.

ACKNOWLEDGEMENT

We thank S. Albright and A. Lasheen in aiding in the understanding of the BLonD code. We thank J. Wei for the wonderful discussion on transition crossing.

ISBN: 978-3-95450-247-9 ISSN: 2673-5490 doi: 10.18429/JACoW-IPAC2024-TUPS01

REFERENCES

[1] F. Willeke, "The hera lepton–proton collider," in *Challenges and Goals for Accelerators in the XXI Century*, ch. Chapter 15, pp. 225–242. doi:10.1142/9789814436403_0015

[2] EIC collaboration, *Electron-Ion Collider at Brookhaven National Laboratory Conceptual Design Report*, 17th ed., pages 183-189, Collider-Acclerator Department, 2020.

[3] E. C. Aschenauer, R. Sassot, and M. Stratmann, "Unveiling the proton spin decomposition at a future electron-ion collider," *Phys. Rev. D*, vol. 92, no. 9, p. 094 030, 2015. doi:10.1103/PhysRevD.92.094030

[4] E.-P. C. Experiment, *Main page — electron-proton/ion collider experiment*, [Online; accessed 10-May-2024], 2024. https://wiki.bnl.gov/EPIC/index.php?title=Main_Page&oldid=1779

[5] M. Woods, *The polarized electron beam for the SLAC Linear Collider*, 1996. doi:10.48550/arXiv.hep-ex/9611006

[6] A. Zelenski, "High-intensity polarized h-(proton), deuteron and 3he++ion source development at bnl.," 2008. https://www.osti.gov/biblio/933081

[7] M. Musgrave *et al.*, "Development of a polarized 3he++ ion source for the eic," 2020, p. 043. doi:10.22323/1.379.0043

[8] *Booster Design Manual*, Brookhaven National Lab., Upton, NY, USA, BNL AGS Internal Rep., 1986, 267 pages.

[9] N. M. Blachman and E. D. Courant, "The Dynamics of a Synchrotron with Straight Sections," *Review of Scientific Instruments*, vol. 20, no. 8, pp. 596–601, 1949. doi:10.1063/1.1741625

[10] R. M. Talman and J. D. Talman, "Electric dipole moment planning with a resurrected bnl alternating gradient synchrotron electron analog ring," *Phys. Rev. Spec. Top. Accel. Beams*, vol. 18, no. 7, p. 074 004, 2015. doi:10.1103/PhysRevSTAB.18.074004

[11] H. Lovelace, J. S. Berg, S. Peggs, S. Polizzo, V. Ptitsyn, and G. Robert-Demolaize, "Transition jump system of the hadron storage ring of the electron ion collider," English, in *Proc. IPAC'23*, Venice, Italy, May 2023, pp. 155–158. doi:10.18429/JACoW-IPAC2023-MOPA056

[12] J.-P. Burnet *et al.*, *Fifty years of the CERN Proton Synchrotron: Volume 1*. CERN, 2011. doi:10.5170/CERN-2011-004

[13] S. Koscielniak, "Near-adiabatic capture of pendulum phase space," TRIUMF, Vancouver, BC, Canada, Tech. Rep. TRI-BN-23-10, 2023.

[14] J. Wei, "Transition crossing in the rhic," 1992. https://www.osti.gov/biblio/5647387

[15] S. Peggs, S. Tepikian, and D. Trbojevic, "A first order matched transition jump at rhic," in *Proc. 15th Particle Accelerator Conf.*, Washington D.C., USA, May 1993, vol. 1, pp. 168–170. doi:10.1109/PAC.1993.308977

[16] K. Johnsen, "Effects Of Non-Linearities On The Phase Transition," in *CERN Symposium on High-Energy Accelerators and Pion Physics*, vol. 1, 1956, pp. 106–111.

[17] H. Timko *et al.*, "Beam longitudinal dynamics simulation studies," *Phys. Rev. Accel. Beams*, vol. 26, no. 11, p. 114 602, 2023. doi:10.1103/PhysRevAccelBeams.26.114602

[18] Accelerator Division, *RHIC:relativistic hadron ion collider configuration manual*, 4th ed., Collider-Accelerator Department, 2006.